*Journal of Structural Geology*, Vol. 13, No. 1, pp. 87 to 96, 1991
Printed in Great Britain

0191-8141/91 $03.00+0.00


# Three-dimensional folding of an embedded viscous layer in pure shear

RAYMOND C. FLETCHER

Center for Tectonophysics and Departments of Geophysics and Geology, Texas A & M University, College Station, TX 77843, U.S.A.

(*Received* 23 *May* 1989; *accepted in revised form* 15 *May* 1990)

**Abstract**—A thick-plate analysis is carried out to first-order in interface slope for three-dimensional folding of a single linear viscous layer of thickness $H$ and viscosity $\eta$ embedded in a uniform viscous medium with viscosity $\eta_1$. Layer and medium are subject to a basic state of homogeneous pure shear with principal directions of strain-rate $x$ and $y$ lying in the plane of the layer. The solution is explicitly carried out for a fold perturbation in interface shape that is symmetric with respect to the principal strain-rate axes, $A\cos(lx)\cos(my)$, but it is shown to apply to an arbitrary perturbation in the $x,y$ plane. The growth rate of the perturbation is found to be

$$dA/dt = -\bar{\varepsilon}_{zz}A + (1-R)\{(1-R^2) - [(1+R^2)(e^k - e^{-k}) + 2R(e^k + e^{-k})]/2k\}^{-1}[(l^2/\lambda^2)\bar{\varepsilon}_{xx} + (m^2/\lambda^2)\bar{\varepsilon}_{yy} - \bar{\varepsilon}_{zz}]A,$$

where $R = \eta_1/\eta$, $k = \lambda H$, $\lambda^2 = l^2 + m^2$, and $\bar{\varepsilon}_{xx}$, $\bar{\varepsilon}_{yy}$, and $\bar{\varepsilon}_{zz}$ are the principal strain-rates of the basic state. The wavenumber of the most rapidly growing perturbation, $\lambda_d$, is the same as that obtained for a cylindrical perturbation ($m = 0$) in a basic state of plane strain ($\bar{\varepsilon}_{yy} = 0$). For maximum rate of shortening parallel to $x$, the cylindrical fold form with axis normal to $x$, $m/l = 0$, grows most rapidly for any ratio of $\bar{\varepsilon}_{yy}/\bar{\varepsilon}_{xx} < 1$. If $\bar{\varepsilon}_{yy} = \bar{\varepsilon}_{xx}$, all fold forms grow at the same rate and in particular, an 'egg-carton' fold form is not preferentially amplified. The velocity field for the perturbing flow consists of a poloidal field, which solely determines the growth of the fold form, and a toroidal field, with non-zero component of vorticity about the axis normal to the layer. The latter is required to satisfy both of the two independent shear traction continuity conditions at interfaces. There is no coupling between the two fields. Three-dimensional fold forms in the Appalachian Plateau province in western Pennsylvania are described.

## INTRODUCTION

THEORETICAL modeling of folds and other tectonic structures has been carried out chiefly for two-dimensional cylindrical structures forming in plane strain. Many folds can be approximated as having cylindrical form, but few are that close to this idealization. Even though individual folds may be approximately cylindrical over much of their length, arrays of folds are fully three-dimensional. Moreover, in many cases, deviations from cylindricity are systematic. For example, the folds may occur in echelon arrays, or they may have characteristic aspect ratios. Hence, potential information in the observations cannot be taken advantage of in the absence of a fully three-dimensional theory. We also have little basis for understanding how cylindrical structures arise in the first place.

A thin-plate theory for three-dimensional folding at low limb-dip has been used by Ghosh (1970) and by Johnson & Page (1976). This treatment is restricted to structures whose wavelengths are large compared to the layer thickness, and to layers which develop a pure fold form in which both surfaces have the same amplitude. However, many single-layer (Sherwin & Chapple 1968, Hudleston & Holst 1984) and large-scale folds above detachment surfaces (Sherwin 1972, Wiltschko & Chapple 1977) do not have large wavelength to thickness ratios. Also, in many structures of interest, such as pinch-and-swell structures (Smith 1975, 1977) and mullions (Smith 1975, 1977, Fletcher 1982), the layers have an important pinch-and-swell component.

As a first step in the study of the initiation and low limb-dip growth of structures arising from flow instability in a layered sequence, including buckling and necking, we consider here the folding of a single isotropic linear viscous layer embedded in a uniform viscous medium. A three-dimensional thick-plate solution is developed along the lines of the two-dimensional analysis (Smith 1975, Fletcher 1977). The present analysis is for a basic state of irrotational pure shear with principal axes of the strain-rate parallel and normal to the plane of the layer. This excludes mean layer-parallel shear (Treagus 1973), but the results can be extended to the case of a mean shear in the plane of the layer.

To motivate the subsequent theoretical treatment, an example of a natural fold array is briefly described.

## A LOW LIMB-DIP FOLD ARRAY IN THE APPALACHIAN PLATEAU PROVINCE

Since the present study is restricted to the analysis of fold growth at low limb-dip, an example of natural folds is taken from the low limb-dip folds of the Appalachian Plateau province in western Pennsylvania. The anticlinal axes of folds in this region are shown in Fig. 1(a) (from Wiltschko & Chapple 1977).

Structural contours on the top of the Oriskany Sandstone (Devonian) for a portion of this region are shown in Fig. 1(b) (from Cate 1964). Only a few structural contours are shown. The −6500′ contour shows the nearly cylindrical anticlines in the center of the map area, the Chestnut Ridge Anticline and the Laurel Hill Anticline to its west. The much higher amplitude Deer

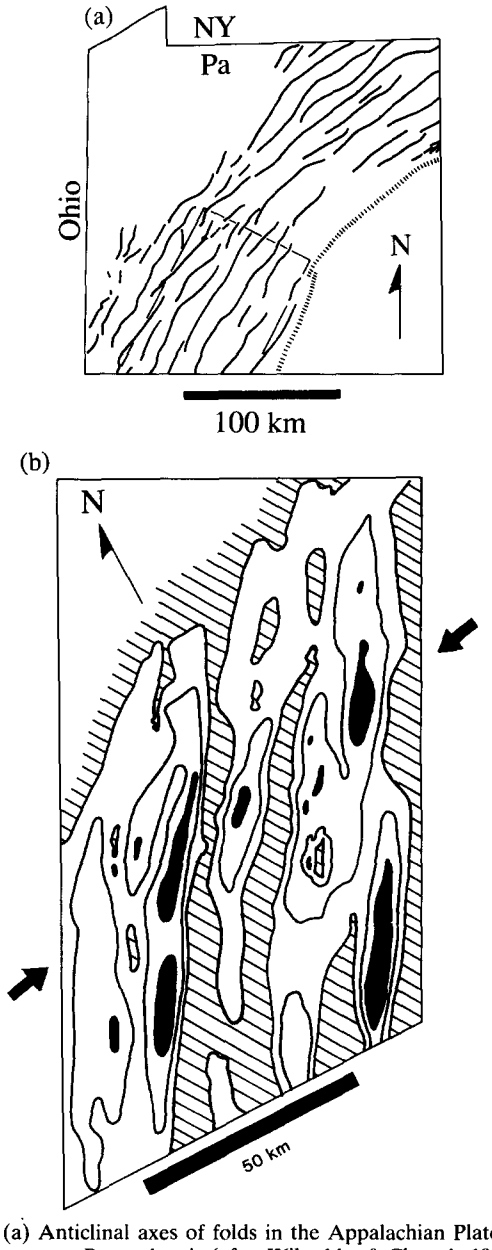


Fig. 1. (a) Anticlinal axes of folds in the Appalachian Plateau province in western Pennsylvania (after Wiltschko & Chapple 1977). The hachured line is the structural front between the Valley-and-Ridge province and the Plateau province. (b) Structural contours on the top of the Oriskany Sandstone in the area of (a) outlined by a solid line (after Cate 1962). The hachured regions lie at or above −6500′; the filled regions lie at or below −7500′; the −7000′ contour within the unshaded regions is approximately at the mean level of the horizon and outlines both anticlines and synclines.

Park Anticline, the easternmost Plateau structure, lies at the eastern edge of the map, and is only indicated by the −6500′ contour on its western flank. The −7000′ contour is close, but somewhat higher than the mean level of the horizon in this area. This contour outlines both synclines and anticlines. The −7500′ contour defines the troughs of the synclines. The maximum elevation of the surface along the crests of the two central anticlines is about −5000′, and the greatest depths in the synclines are at about −8500′, but these higher and lower contours are not shown. To the northwest, the mean level of the horizon rises, so that additional contours would be required to clearly delineate the folds there.

Qualitative features of the three-dimensional fold form include culminations and saddles along the trend of an anticline and depressions and saddles along the trend of a syncline. Folds may terminate, as indicated in the map of anticlinal axes (Fig. 1a), but the sparseness of contours makes this difficult to see in Fig. 1(b). The trends of the folds show subtle variations, and there is some suggestion of an echelon arrangement of some folds. A striking, if subdued, feature is an E-trending series of synclinal depressions and at least one prominent anticlinal saddle that crosses the central part of the area. This is indicated by the arrows in Fig. 1(b). Indications of this secondary structural trend are seen to the south and north.

Most of the systematic features seen in the contour map can be replicated by adding two periodic components in a representation of the height of a folded surface above a mean horizontal datum. For example, consider the surface

$$\zeta(x,y) = A\cos(lx) + B\cos(l'x'), \qquad (1a)$$

where the $x'$ axis makes an angle $\beta$ with the $x$ axis, and, consequently,

$$x' = x\cos\beta + y\sin\beta. \qquad (1b)$$

A surface of this form plotted in Fig. 2 represents the sum of a sinusoidal wave with amplitude $A = 1$ (in arbitrary units) and a N–S axis, plus an obliquely-oriented sinusoidal wave with the same wavelength and amplitude $B = 0.25$, whose axis trends N30°E ($\beta = -30°$). This surface shows anticlinal culminations or synclinal depressions and saddles along the fold axes. It also shows fluctuations in the axial trends which correspond to an echelon arrangement of successive anticlinal culminations or synclinal depressions. Finally,

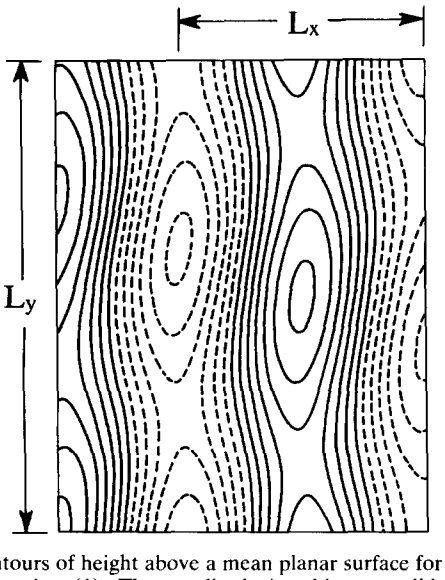


Fig. 2. Contours of height above a mean planar surface for the form given in equation (1). The amplitude is arbitrary; solid lines are positive and dashed lines are negative relative to the mean level of the surface. $L_x$ and $L_y$ are the fold wavelengths in the $x$ and $y$ directions, respectively.

the synclinal minima and anticlinal saddles, and the anticlinal maxima and synclinal saddles, line up along the N30°E trend. The pattern therefore duplicates, in a sharper, more idealized way, the qualitative features seen in the natural fold array from the Appalachian Plateau province.

In interpreting the natural fold pattern shown in Fig. 1(b), it might be supposed that the initial irregularity selectively amplified in the low limb-dip phase of folding had a pronounced and possibly regular E–W structure. This pre-existing structure might have been the result of a prior episode of shortening with a more northeasterly orientation. (No other evidence for such a sequence of events is known to the author.) The evolving fold form can be idealized by that given in equation (1a), and the evolution of such a form in E–W shortening can then be considered. For example, will the shortening cause further significant amplification of the secondary component, thereby insuring its preservation in the final structure?

## ANALYSIS OF THICK-PLATE FOLDING IN THREE DIMENSIONS AT LOW LIMB-DIP

### *Form of perturbed surface*

Let the form of the upper surface of a layer of thickness $2h$ be expressed as the height above the central plane of the layer. Then the surface form (1) can be expanded in the principal co-ordinates $x$ and $y$ as

$$\begin{aligned}\zeta(x,y) = h &+ A\cos(lx)\\ &+ B\cos(l'\cos\beta x)\cos(l'\sin\beta y)\\ &- B\sin(l'\cos\beta x)\sin(l'\sin\beta y).\end{aligned} \tag{2}$$

We seek a solution for the perturbing flow associated with a shape perturbation of this type that is accurate to first-order in the local slope of the surface. The three components describing the shape perturbation in (2) are orthogonal. Therefore, they give rise to linearly independent perturbing flows, which evolve independently of each other. The solution for the first component in the shape perturbation may be obtained from the two-dimensional theory, with attention to the possible non-zero value of $\bar{\varepsilon}_{yy}$. Given a solution for the second component, the solution for the third component is obtained by applying appropriate phase shifts in $x$ and $y$. It suffices then, to obtain a solution for a surface of the form

$$\zeta(x,y) = h + A\cos(lx)\cos(my). \tag{3}$$

The first component then corresponds to the case $m = 0$.

### *Perturbing flow*

The method of analysis used here follows, in its general approach, that used by Smith (1975) and Fletcher (1977) for the two-dimensional problem.

A layer of thickness $H = 2h$ and viscosity $\eta$ is embedded in a medium with viscosity $\eta_1$. Both are subject to a basic state of uniform pure shear with principal strain-rates $\bar{\varepsilon}_{xx}$, $\bar{\varepsilon}_{yy}$ and $\bar{\varepsilon}_{zz}$. The principal axes $x$ and $y$ lie in the plane of the layer, and $z$ lies normal to it. The non-zero stresses associated with the basic state are, in the layer,

$$\begin{aligned}\bar{\sigma}_{xx} - \bar{\sigma}_{zz} &= 4\eta(\bar{\varepsilon}_{xx} - \bar{\varepsilon}_{zz})\\ \bar{\sigma}_{yy} - \bar{\sigma}_{zz} &= 4\eta(\bar{\varepsilon}_{yy} - \bar{\varepsilon}_{zz})\\ \bar{\sigma}_{xx} - \bar{\sigma}_{yy} &= 4\eta(\bar{\varepsilon}_{xx} - \bar{\varepsilon}_{yy})\end{aligned} \tag{4a}$$

and in the overlying medium,

$$\begin{aligned}\bar{\sigma}^{(1)}_{xx} - \bar{\sigma}_{zz} &= 4\eta_1(\bar{\varepsilon}_{xx} - \bar{\varepsilon}_{zz})\\ \bar{\sigma}^{(1)}_{yy} - \bar{\sigma}_{zz} &= 4\eta_1(\bar{\varepsilon}_{yy} - \bar{\varepsilon}_{zz})\\ \bar{\sigma}^{(1)}_{xx} - \bar{\sigma}^{(1)}_{yy} &= 4\eta_1(\bar{\varepsilon}_{xx} - \bar{\varepsilon}_{yy}),\end{aligned} \tag{4b}$$

where $\bar{\sigma}_{xx}$, $\bar{\sigma}_{yy}$ and $\bar{\sigma}_{zz}$ are the components of the stress, and the superscript or subscript 1 refers to the upper medium. The stresses are the same in the lower medium, denoted by index 2, since $\eta_2 = \eta_1$.

If the layer surfaces are perfectly plane, the basic state of flow exactly satisfies the boundary conditions on the continuity of surface tractions and velocity components.

We now perturb the shape of the layer to a pure fold form, with the upper surface given by (3) and the lower surface by

$$\zeta^*(x,y) = -h + A\cos(lx)\cos(my). \tag{5}$$

The amplitude of the fold perturbation is $A$, and its wavelengths in the $x$ and $y$ directions are $L_x = 2\pi/l$ and $L_y = 2\pi/m$. The perturbation given by equations (3) and (5) has its symmetry axes coincident with the principal axes of the strain-rate in the plane of the layer. Height contours for the fold form are shown in Fig. 3 for the case $L_x/L_y = 0.5$.

The basic state will no longer satisfy all the boundary conditions on the surfaces $\zeta$ and $\zeta^*$, and it is necessary to introduce a perturbing flow with velocity components $\tilde{u}$,

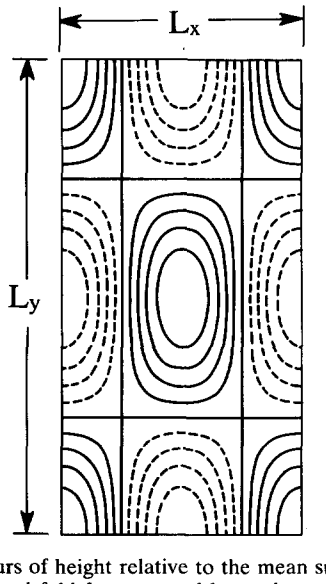


Fig. 3. Contours of height relative to the mean surface level for the three-dimensional fold form treated here; the amplitude is given in arbitrary units; solid lines are positive and dashed lines are negative relative to the mean level of the surface.

$\tilde{v}$ and $\tilde{w}$, and stress components $\tilde{\sigma}_{xx}$, $\tilde{\sigma}_{yy}$, $\tilde{\sigma}_{zz}$, $\tilde{\sigma}_{yz}$, $\tilde{\sigma}_{zx}$ and $\tilde{\sigma}_{xy}$.

In general, there will be six independent boundary conditions at each interface. Three of these express the continuity of the components of stress normal to and tangent to the interface. In the present case, a welded interface is assumed, and the other three boundary conditions express the continuity of the three components of velocity. Because of the symmetry of the present fold configuration, only the boundary conditions at the upper surface need be considered, and there will be a corresponding simplification in the general form of the solution.

The basic-state velocity is already continuous at the interface, so that the components of the perturbing velocity are required to be continuous. To take advantage of symmetry, the co-ordinate origin for the flow in the layer is taken at its mid-plane. It is more convenient to take the co-ordinate origin for the flow in the upper medium at the mean level of the upper interface. To first-order in the maximum slope (Fletcher 1977) the velocity boundary conditions then reduce to

$$\begin{aligned} \tilde{u}(x,y,h) &\cong \tilde{u}^{(1)}(x,y,0) \\ \tilde{v}(x,y,h) &\cong \tilde{v}^{(1)}(x,y,0) \\ \tilde{w}(x,y,h) &\cong \tilde{w}^{(1)}(x,y,0). \end{aligned} \tag{6}$$

Let $s$, $t$ and $n$ denote three axes locally tangent and normal to the interface (Fig. 4). The stress boundary conditions at the upper surface are then

$$\begin{aligned} \sigma_{nn}(x,y,\zeta) &= \sigma_{nn}^{(1)}(x,y,\zeta) \\ \sigma_{ns}(x,y,\zeta) &= \sigma_{ns}^{(1)}(x,y,\zeta) \\ \sigma_{nt}(x,y,\zeta) &= \sigma_{nt}^{(1)}(x,y,\zeta). \end{aligned} \tag{7}$$

The axes $n$ and $s$ are chosen to lie in a vertical plane, containing the $z$-axis, so that the remaining axis $t$ is horizontal. Unit vectors in the directions of $s$, $t$ and $n$ are then, to first-order in the maximum slope $\lambda A$ given by

$$\begin{aligned} s &\cong T^{-1}[t_2T, \quad -t_1T, \quad s_3T] \\ t &\cong T^{-1}[t_1T, \quad t_2T, \quad 0] \\ n &\cong [-\partial\zeta/\partial x, \quad -\partial\zeta/\partial y, \quad 1], \end{aligned} \tag{8a}$$

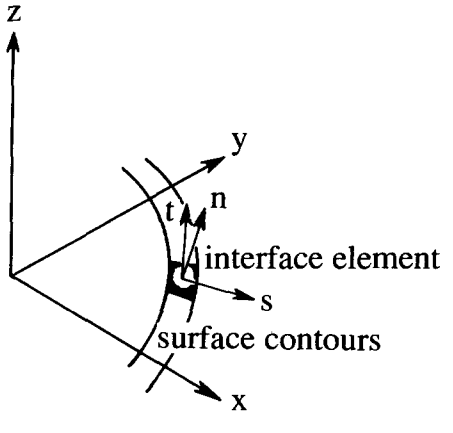


Fig. 4. Local co-ordinates $s$, $t$ and $n$, where $s$ and $t$ are tangent to the interface, and $n$ is normal to it.

where

$$\begin{aligned} t_1T &= -m\cos(lx)\sin(my) \\ t_2T &= l\sin(lx)\cos(my) \\ s_3T &= -[m^2\cos^2(lx)\sin^2(my) \\ &\quad + l^2\sin^2(lx)\cos^2(my)]A \end{aligned}$$

and

$$T = [m^2\cos^2(lx)\sin^2(my) + l^2\sin^2(lx)\cos^2(my)]^{1/2}. \tag{8b}$$

Since the components of these vectors are the direction cosines between the axes $s$, $t$ and $n$ and the axes $x$, $y$ and $z$, the tensor transformation carried out to first-order in the slope and taking into account the non-vanishing basic-state stresses yields

$$\begin{aligned} \sigma_{ns} &\cong (t_2T)\tilde{\sigma}_{xz} - (t_1T)\tilde{\sigma}_{yz} - t_2T(\partial\zeta/\partial x)\tilde{\sigma}_{xx} \\ &\quad + t_1T(\partial\zeta/\partial y)\tilde{\sigma}_{yy} - s_3T\tilde{\sigma}_{zz} \\ \sigma_{nt} &\cong (t_1T)\tilde{\sigma}_{xz} + (t_2T)\tilde{\sigma}_{yz} - t_1T(\partial\zeta/\partial x)\tilde{\sigma}_{xx} \\ &\quad - t_2T(\partial\zeta/\partial y)\tilde{\sigma}_{yy} \\ \sigma_{nn} &\cong \sigma_{zz}. \end{aligned} \tag{9}$$

The expressions for $\sigma_{ns}^{(1)}$, . . . are obtained by adding superscripts to all stress components in (9). Note that $\tilde{\sigma}_{zz}^{(1)} = \tilde{\sigma}_{zz}$.

When the expressions (9) are substituted into the continuity conditions (7), it is found that the first two conditions can be reduced to the two much simpler conditions

$$\begin{aligned} \tilde{\sigma}_{xz}(x,y,h) - \sigma_{xz}^{(1)}(x,y,0) &= 4\eta(1-R)\tilde{\varepsilon}_{xx}\partial\zeta/\partial x \\ \tilde{\sigma}_{yz}(x,y,h) - \sigma_{yz}^{(1)}(x,y,0) &= 4\eta(1-R)\tilde{\varepsilon}_{xx}\partial\zeta/\partial y, \end{aligned} \tag{10a}$$

where

$$\tilde{\sigma}_{xx} - \tilde{\sigma}_{xx}^{(1)} = 4(\eta - \eta_1)\tilde{\varepsilon}_{xx} \quad \text{and} \quad \tilde{\sigma}_{yy} - \tilde{\sigma}_{yy}^{(1)} = 4(\eta - \eta_1)\tilde{\varepsilon}_{yy}$$

have been used, and $R = \eta_1/\eta$. The third condition in (7) yields

$$\tilde{\sigma}_{zz}(x,y,h) - \tilde{\sigma}_{zz}^{(1)}(x,y,0) = 0. \tag{10b}$$

The solution accordingly requires the determination of the form of the perturbing flow which satisfies the six boundary conditions (6) and (10).

The separable form of the perturbing velocity components for the two-dimensional plane flow problem is

$$\begin{aligned} \tilde{u} &= -(1/l)\mathrm{d}W/\mathrm{d}z\sin(lx) \\ \tilde{v} &= 0 \\ \tilde{w} &= W(z)\cos(lx). \end{aligned} \tag{11}$$

These satisfy the condition of incompressibility

$$\partial u/\partial x + \partial v/\partial y + \partial w/\partial z = 0. \tag{12}$$

The form (11) provides a solution for the special case of an interface of the form (3) that is cylindrical ($m = 0$). The extension of this solution to the three-dimensional case is accomplished (Bisshop 1960, Biot 1966) by writing

$$\tilde{u} = (l/\lambda^2)\mathrm{d}W/\mathrm{d}z(\partial\Phi/\partial x)$$
$$\tilde{v} = (m/\lambda^2)\mathrm{d}W/\mathrm{d}z(\partial\Phi/\partial y) \quad (13)$$
$$\tilde{w} = W(z;\lambda)\Phi(x,y),$$

where $\lambda^2 = l^2 + m^2$, and $\Phi(x,y)$ is a harmonic function

$$\partial^2\Phi/\partial x^2 + \partial^2\Phi/\partial y^2 = -\lambda^2\Phi. \quad (14)$$

For the interface shape (3), the appropriate choice of harmonic function is

$$\Phi = \cos(lx)\cos(my). \quad (15)$$

Substitution of (13), with (14) into the equations

$$\eta\nabla^2 u = \partial p/\partial x$$
$$\eta\nabla^2 v = \partial p/\partial y \quad (16)$$
$$\eta\nabla^2 w = \partial p/\partial z,$$

where $p$ is the pressure, yields after a standard development

$$W = [\mathrm{A} + \mathrm{B}(\lambda z - 1)]\mathrm{e}^{\lambda z} - [\mathrm{C} + \mathrm{D}(\lambda z + 1)]\mathrm{e}^{-\lambda z} \quad (17)$$

where A, B, C and D are arbitrary constants. The velocity components are then

$$\begin{aligned}\tilde{u} &= -(l/\lambda)\{[\mathrm{A} + \mathrm{B}(\lambda z)]\mathrm{e}^{\lambda z} \\ &\quad + [\mathrm{C} + \mathrm{D}(\lambda z)]\mathrm{e}^{-\lambda z}\}\sin(lx)\cos(my) \\ \tilde{v} &= -(m/\lambda)\{[\mathrm{A} + \mathrm{B}(\lambda z)]\mathrm{e}^{\lambda z} \\ &\quad + [\mathrm{C} + \mathrm{D}(\lambda z)]\mathrm{e}^{-\lambda z}\}\cos(lx)\sin(my) \\ \tilde{w} &= \{[\mathrm{A} + \mathrm{B}(\lambda z - 1)]\mathrm{e}^{\lambda z} \\ &\quad - [\mathrm{C} + \mathrm{D}(\lambda z + 1)]\mathrm{e}^{-\lambda z}\}\cos(lx)\cos(my).\end{aligned} \quad (18a)$$

The stress components are

$$\begin{aligned}\tilde{\sigma}_{xx} &= -2\eta\lambda\{\{(l^2/\lambda^2)\{[\mathrm{A} + \mathrm{B}(\lambda z)]\mathrm{e}^{\lambda z} \\ &\quad + [\mathrm{C} + \mathrm{D}(\lambda z)]\mathrm{e}^{-\lambda z}\} \\ &\quad + (\mathrm{Be}^{\lambda z} - De^{-\lambda z})\}\}\cos(lx)\cos(my) \\ \tilde{\sigma}_{yy} &= -2\eta\lambda\{\{(m^2/\lambda^2)\{[\mathrm{A} + \mathrm{B}(\lambda z)]\mathrm{e}^{\lambda z} \\ &\quad + [\mathrm{C} + \mathrm{D}(\lambda z)]\mathrm{e}^{-\lambda z}\} \\ &\quad + (\mathrm{Be}^{\lambda z} - \mathrm{De}^{-\lambda z})\}\}\cos(lx)\cos(my) \\ \tilde{\sigma}_{zz} &= 2\eta\lambda\{[\mathrm{A} + \mathrm{B}(\lambda z - 1)]\mathrm{e}^{\lambda z} \\ &\quad + [\mathrm{C} + \mathrm{D}(\lambda z + 1)]\mathrm{e}^{-\lambda z}\}\cos(lx)\cos(my) \\ \tilde{\sigma}_{xy} &= -2\eta(lm/\lambda)\{[\mathrm{A} + \mathrm{B}(\lambda z)]\mathrm{e}^{\lambda z} \\ &\quad - [\mathrm{C} + \mathrm{D}(\lambda z)]\mathrm{e}^{-\lambda z}\}\sin(lx)\sin(my) \\ \tilde{\sigma}_{xz} &= -2\eta l\{[\mathrm{A} + \mathrm{B}(\lambda z)]\mathrm{e}^{\lambda z} \\ &\quad - [\mathrm{C} + \mathrm{D}(\lambda z)]\mathrm{e}^{-\lambda z}\}\sin(lx)\cos(my) \\ \tilde{\sigma}_{yz} &= -2\eta m\{[\mathrm{A} + \mathrm{B}(\lambda z)]\mathrm{e}^{\lambda z} \\ &\quad - [\mathrm{C} + \mathrm{D}(\lambda z)]\mathrm{e}^{-\lambda z}\}\cos(lx)\sin(my).\end{aligned} \quad (18b)$$

Expressions for the velocity and stress components in the upper medium may be obtained by affixing the subscript 1 to the coefficients and to the viscosity in (18a) and (18b). Since the flow must vanish in the upper medium as $z \to \infty$, $\mathrm{A}_1 = \mathrm{B}_1 = 0$. For the pure fold form given by (3) and (5), the symmetry of the flow within the layer requires that $\tilde{w}(x,y,-z) = \tilde{w}(x,y,z)$, which implies that

$$\mathrm{C} = -\mathrm{A}$$
$$\mathrm{D} = \mathrm{B}. \quad (19)$$

Thus, taking these conditions into account, only the four arbitrary coefficients A, B, $\mathrm{C}_1$ and $\mathrm{D}_1$ are available to satisfy the six boundary conditions at the upper interface. It may be verified that the boundary conditions can only be satisfied in the special case $\bar{\varepsilon}_{yy} = \bar{\varepsilon}_{xx}$ and $m = l$. To obtain a solution for the general case, an independent solution supplying two additional arbitrary constants for each medium is therefore required.

It may be noted that the velocity field (13) has the special property that the $z$ component of the vorticity vanishes, $\omega_z = 1/2(\partial v/\partial x - \partial u/\partial y) = 0$. A solution of the form

$$\tilde{u} = \partial\Psi/\partial y$$
$$\tilde{v} = -\partial\Psi/\partial x \quad (20)$$
$$\tilde{w} = 0$$

satisfies the condition of incompressibility (12) and gives a non-zero value of $\omega_z$. It is required here that $\Psi$ also be separable in its $z$-dependence and $x,y$-dependence. Substitution of (20) into (16) yields

$$\Psi = (\mathrm{Me}^{\lambda z} + \mathrm{Ne}^{-\lambda z})\sin(lx)\sin(my), \quad (21)$$

where M and N are arbitrary constants. The form of the $x,y$-dependence of $\Psi$ for a perturbation of the form (3) has been deduced from symmetry arguments. The general expressions for the non-zero velocity and stress components are

$$\tilde{u} = m(\mathrm{Me}^{\lambda z} + \mathrm{Ne}^{-\lambda z})\sin(lx)\cos(my)$$
$$\tilde{v} = -l(\mathrm{Me}^{\lambda z} + \mathrm{Ne}^{-\lambda z})\cos(lx)\sin(my) \quad (22a)$$

and

$$\begin{aligned}\tilde{\sigma}_{xx} &= 2\eta lm(\mathrm{Me}^{\lambda z} + \mathrm{Ne}^{-\lambda z})\cos(lx)\cos(my) \\ \tilde{\sigma}_{yy} &= -2\eta lm(\mathrm{Me}^{\lambda z} + \mathrm{Ne}^{-\lambda z})\cos(lx)\cos(my) \\ \tilde{\sigma}_{zz} &= 0 \\ \tilde{\sigma}_{xy} &= 2\eta(l^2 - m^2)(\mathrm{Me}^{\lambda z} + \mathrm{Ne}^{-\lambda z})\sin(lx)\sin(my) \\ \tilde{\sigma}_{xz} &= 2\eta\lambda m(\mathrm{Me}^{\lambda z} - \mathrm{Ne}^{-\lambda z})\cos(lx)\cos(my) \\ \tilde{\sigma}_{yz} &= -2\eta\lambda l(\mathrm{Me}^{\lambda z} - \mathrm{Ne}^{-\lambda z})\cos(lx)\cos(my).\end{aligned} \quad (22b)$$

From (22a), the $z$ component of the vorticity in the layer is

$$\tilde{\omega}_z = \lambda^2(\mathrm{Me}^{\lambda z} + \mathrm{Ne}^{-\lambda z})\sin(lx)\sin(my). \quad (23)$$

By symmetry, $\omega_z$ must also be an even function of $z$ for the fold configuration studied, and hence,

$$\mathrm{N} = \mathrm{M}. \quad (24)$$

The vanishing of the perturbing flow in the upper medium as $z \to \infty$ requires that

$$\mathrm{M}_1 = 0. \quad (25)$$

The full expressions for the velocity and stress components in the layer are therefore obtained by adding (22a) to (18a) and (22b) to (18b), respectively, and then applying the restrictions (19) and (24). The full expressions for the upper medium are similarly obtained. The restrictions reduce the arbitary constants in these solutions to six: A, B, M, $C_1$, $D_1$ and $N_1$. Application of the six boundary conditions (6) and (10) then yield

$$\begin{aligned}
&-(l/\lambda)[A(e^{\lambda h} - e^{-\lambda h}) + B(\lambda h)(e^{\lambda h} + e^{-\lambda h})] \\
&\qquad + mM(e^{\lambda h} - e^{-\lambda h}) = -(l/\lambda)C_1 + mN_1 \\
&-(m/\lambda)[A(e^{\lambda h} - {}^{-\lambda h}) + B(\lambda h)(e^{\lambda h} + e^{-\lambda h})] \\
&\qquad - lM(e^{\lambda h} - e^{-\lambda h}) = -(m/\lambda)C_1 - lN_1 \\
&A(e^{\lambda h} + e^{-\lambda h}) + B[(\lambda h)(e^{\lambda h} - e^{-\lambda h}) - (e^{\lambda h} + e^{-\lambda h})] \\
&\qquad = -(C_1 + D_1) \qquad (26) \\
&A(e^{\lambda h} - e^{-\lambda h}) + B[\lambda h(e^{\lambda h} + e^{-\lambda h}) \\
&\qquad - (e^{\lambda h} - e^{-\lambda h})] - R(C_1 + D_1) = 0 \\
&A(e^{\lambda h} + e^{-\lambda h}) + B\lambda h(e^{\lambda h} - e^{-\lambda h}) + RC_1 \\
&\qquad = (1 - R)[(l^2/\lambda^2)\bar{\varepsilon}_{xx} + (m^2/\lambda^2)\bar{\varepsilon}_{yy} - \bar{\varepsilon}_{zz}]A \\
&M(e^{\lambda h} + e^{-\lambda h}) + RN_1 = -2(lm/\lambda^3)(1 - R)(\bar{\varepsilon}_{xx} - \bar{\varepsilon}_{yy})A.
\end{aligned}$$

The first pair in (26) may be re-arranged to give

$$\begin{aligned}
A(e^{\lambda h} - e^{-\lambda h}) + B(\lambda h)(e^{\lambda h} + e^{-\lambda h}) &= -C_1 \\
M(e^{\lambda h} - e^{-\lambda h}) &= N_1.
\end{aligned} \qquad (27)$$

The relations (26) determine the six arbitrary constants A, B, $C_1$, $D_1$, M and $N_1$. Taking (27) into account, it may be seen that the first four constants are independently determined from four of the relations, and the remaining two constants, M and $N_1$, are determined from the remaining two relations. Thus, to the present order of approximation, the two flows are neither coupled in the governing equations nor the boundary conditions.

## DISCUSSION

### *Generality of the solution*

The two velocity fields (18a) and (22a) may be termed the poloidal flow and the toroidal flow, respectively, because of their properties referred to the special coordinate direction $z$ normal to layering. The $z$ component of the vorticity, $\omega_z$, vanishes for the poloidal field. The toroidal flow has non-vanishing $\omega_z$, and if $\omega_z$ does vanish, the toroidal field vanishes as well. For a layered configuration of isotropic, linear viscous fluids, the poloidal and toroidal flows are neither coupled through the governing equations nor through the boundary conditions.

The general form of the solution given here may be applied to solve all problems involving layers of isotropic viscous fluid. In the case of density instability alone, the toroidal flow vanishes, and the velocity field is purely poloidal (Biot 1966).

### *Growth rate of a three-dimensional fold perturbation*

The rate of growth of the amplitude is given, to the present order of approximation, by

$$dA/dt \cong \bar{\varepsilon}_{zz}A + \tilde{w}(0,0,h). \qquad (28)$$

Substitution from (18a), using (19) and the values of the constants A and B obtained from the relations (26) yields

$$dA/dt \cong \bar{\varepsilon}_{zz}A - (q/2)[l^2/\lambda^2)\bar{\varepsilon}_{xx} + (m^2/\lambda^2)\bar{\varepsilon}_{yy} - \bar{\varepsilon}_{zz}]A, \qquad (29)$$

where

$$\begin{aligned}
q = -2(1 - R)\{(1 - R^2) - [(1 + R^2)(e^k - e^{-k}) \\
+ 2R(e^k + e^{-k})]/2k\}^{-1}
\end{aligned}$$

and $k = \lambda H$. For $k \ll 1$, $q$ has the approximate form obtained from the thin-plate analysis (Ghosh 1970, Johnson & Page 1976)

$$q = 12/(k^2 + R/k). \qquad (30)$$

Hence, with the exception of the thick-plate expression for $q$, which has been already obtained in Fletcher (1977), the relation (29) for the growth rate of a three-dimensional perturbation is identical to that obtained by Ghosh (1970) and Johnson & Page (1976).

The dominant wavenumber $k_d$, which maximizes $q$ in (29), is the same as that determined for the case of a cylindrical perturbation in plane strain. Here, however, the growth rate depends also on the fold aspect ratio $L_x/L_y = m/l$, through the quantity in square brackets in (29). Let shortening take place parallel to $x$, so that $\bar{\varepsilon}_{xx} < 0$, and if shortening takes place also in the $y$ direction, let $\bar{\varepsilon}_{xx} \leq \bar{\varepsilon}_{yy}$. The function

$$\begin{aligned}
E &= -[(l^2/\lambda^2)\bar{\varepsilon}_{xx} + (m^2/\lambda^2)\bar{\varepsilon}_{yy} - \bar{\varepsilon}_{zz}]/|\bar{\varepsilon}_{xx}| \\
&= (l^2/\lambda^2 + 1) + (m^2/\lambda^2 + 1)\bar{\varepsilon}_{yy}/\bar{\varepsilon}_{xx}
\end{aligned} \qquad (31)$$

is then a measure of the dependence of the folding rate on the fold aspect aspect ratio; larger $E$ means a larger folding rate. The strain rate ratio $\bar{\varepsilon}_{yy}/\bar{\varepsilon}_{xx} \leq 1$ is positive if shortening takes place in the $y$ direction and $\bar{\varepsilon}_{yy} < 0$, or negative if extension takes place parallel to $y$. By inspection, recalling that $\lambda^2 = l^2 + m^2$, it can be seen that $E$ is maximized for any allowable ratio $\bar{\varepsilon}_{yy}/\bar{\varepsilon}_{xx} < 1$ by the choice $m = 0$, or for a cylindrical fold form with axis normal to the $x$ direction of maximum shortening rate. For the special case $\bar{\varepsilon}_{yy}/\bar{\varepsilon}_{xx} = 1$, the growth rate is independent of the fold form.

This result is not consistent with one reported by Johnson & Page (1976) for the buckling of a thin elastic plate. With suitable re-interpretation of quantities, the formal solution to the elastic problem should agree with the solution for the folding of a viscous layer in a viscous medium. Johnson & Page (1976) obtain a result that is equivalent to the statement that for any positive ratio of the strain rates $\bar{\varepsilon}_{xx}/\bar{\varepsilon}_{yy}$, the growth rate is maximized for a non-zero aspect ratio $L_x/L_y = m/l$. This identifies a particular fold aspect ratio with a particular strain-rate ratio. This plausible result, however, is not correct. The

form to be maximized (Johnson & Page 1976, equation 26f) is identical to (31) here. The error arises in the expansion of this quantity, which is given on the right-hand side of Johnson's & Page's equation (26f). Since the result in question can be derived from the published form of their equation (26f), the error is not a typographical error. The correct expression on the right-hand side of their (26f) should have as its denominator $[(L_x/L_y)^2 + 1]^2$.

For a basic state of plane strain, $\bar{\varepsilon}_{yy} = 0$, and $\bar{\varepsilon}_{zz} = \bar{\varepsilon}_{xx}$, (31) reduces to

$$E = [1 + (m/l)^2]^{-1} + 1. \tag{32}$$

This is maximized for the cylindrical fold form with axis normal to the direction of shortening, $m/l = 0$, for which $E = 2$, and decreases monotonically but slowly as $m/l$ increases. Remarkably, it falls to only $E = 1$ for the extreme case $m/l \to \infty$, which corresponds to a cylindrical fold form whose axis lies *parallel* to the direction of shortening. In comparing these two cases, recall that if the amount of amplification for some increment of shortening is 100 for $E = 2$, that for $E = 1$ will be only 10. When the axis is parallel to the shortening direction in plane strain, there is vertical extension, but no shortening normal to the fold axis.

Watkinson (1975) has conducted experiments to produce folding in the case $\bar{\varepsilon}_{zz} = 0$, whence $\bar{\varepsilon}_{yy} = -\bar{\varepsilon}_{xx}$. In this case,

$$E = [(l^2/\lambda^2) - (m^2/\lambda^2)]. \tag{33}$$

The maximum rate of amplification occurs for the cylindrical fold form with axis normal to the shortening direction, for which $E = 1$. A fold form with aspect ratio $L_x/L_y = 1$ is not amplified, except kinematically, and fold forms with $L_x/L_y < 1$ decay.

For the special basic state $\bar{\varepsilon}_{yy} = \bar{\varepsilon}_{xx}$,

$$E = (l^2 + m^2)/\lambda^2 + 2 = 3, \tag{34}$$

and the rate of amplification is the same for all fold forms. In particular, the 'egg-carton' form, $L_y = L_x$, is not preferentially amplified. Since $E$ has been chosen to scale with $|\bar{\varepsilon}_{xx}|$, the addition of shortening parallel to $y$ necessarily augments the strength of instability, as we have already seen for the cylindrical fold form.

The general relationship can be shown by contours of $E$ in the space of $L_x/L_y$ and $\bar{\varepsilon}_{yy}/\bar{\varepsilon}_{xx}$ (Fig. 5). To summarize these results, whatever the ratio $\bar{\varepsilon}_{yy}/\bar{\varepsilon}_{xx}$, the growth rate is maximized for a cylindrical fold form with axis normal to the direction of maximum shortening. The differential in growth rate with varying $m/l$ is maximized in a basic state of plane strain. It disappears for the basic state $\bar{\varepsilon}_{yy} = \bar{\varepsilon}_{xx} < 0$, in which all fold forms grow at an equal rate. For $\bar{\varepsilon}_{yy} > 0$, fold forms with their long axis in the direction of shortening, $L_x/L_y < 1$, begin to decay, first at very large aspect ratio, and then at smaller ratio as $\bar{\varepsilon}_{yy}$ increases.

The chief factors influencing the aspect ratio of three-dimensional folds formed at low limb-dip are therefore: (i) the general preference for cylindrical fold forms; (ii) the variation in this effect with the in-plane strain-rates; and (iii) the nature of the initial perturbation. A selectivity for fold form is thus present, in contrast to the case with density instability (Biot 1966) in which all forms have the same growth rate, but the selectivity does not favor a finite aspect $L_x/L_y$ at each value of $\bar{\varepsilon}_{yy}/\bar{\varepsilon}_{xx}$. Further insight into the development of three-dimensional fold form will likely require the simulation of fold arrays, as in the case of cylindrical fold arrays (Fletcher & Sherwin 1977).

*Treatment of arbitrary three-dimensional fold forms*

The symmetry restriction imposed in carrying out the formal analysis is not, in fact, a restriction at all, and the present results apply to the amplification of any three-dimensional fold form.

Any three-dimensional surface form can be represented by the summation of expressions of the form

$$\zeta(x,y) = A\cos(lx)\cos(my) + B\cos(lx)\sin(my) + C\sin(lx)\cos(my) + D\sin(lx)\sin(my), \tag{35}$$

where $A$, $B$, $C$ and $D$ are arbitrary amplitudes. The summation is over all appropriate wavenumbers $l$ and $m$. More precisely, a surface form within a finite rectangular region of the $x,y$ plane can be represented by a double sum over an infinite but discrete set of wavenumbers. For an unbounded region, the summation is replaced by a Fourier integral.

Given the explicit solution for the first term, $A\cos(lx)\cos(my)$, that for the other terms are obtained by noting that the first term can be converted to any of the others merely by a shift in co-ordinate origin of $\pm\pi/2$ in the arguments $lx$ or $my$. At the same time, the forms described by each of the four terms in (35) evolve independently, since the products are orthogonal on the $x,y$ plane. The growth rates for each depend solely on the parameters $\lambda^2 = l^2 + m^2$ and $m/l$, and, hence, are identical.

These remarks are sufficient to indicate the full generality of the present solution, for the boundary-value

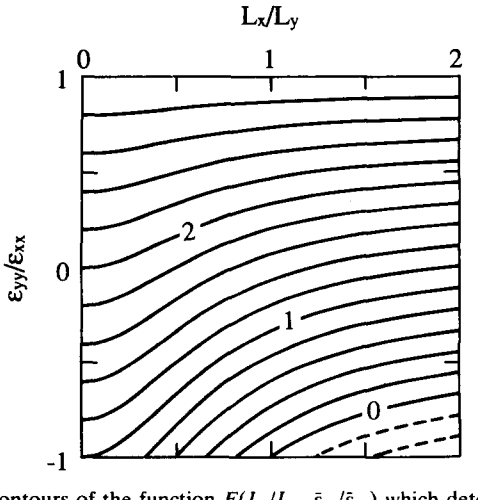


Fig. 5. Contours of the function $E(L_x/L_y, \bar{\varepsilon}_{yy}/\bar{\varepsilon}_{xx})$ which determines the rate of fold amplification as a function of fold aspect ratio $L_x/L_y$ and strain-rate ratio $\bar{\varepsilon}_{yy}/\bar{\varepsilon}_{xx}$ at a given wavenumber $\lambda$.

problem considered here. However, discussion of simple cases will serve to illustrate some practical applications.

The notion of a 'fold wavelength' is common in the literature. However, folds and similar structures do not have wavelengths in any rigorous sense because they are not periodic structures: they do not possess long-range order. They do have a characteristic spacing. In the case of approximately cylindrical single-layer folds, which are the only structure to be studied in any detail (Sherwin & Chapple 1968, Hudleston & Holst 1984), sections cut normal to the fold axis show a regularity that is usefully represented on a histogram of crest-to-crest fold arc lengths normalized by the layer thickness, $L/H$. Histograms of $L/H$ generally show a prominent maximum, but there is generally substantial dispersion about the mean value (Hudleston & Holst 1984). The regularity resulting from the folding process is a short-range order, so that the average $\bar{L}$ will be a good estimate of the next nearest fold crest, but $N\bar{L}$ will not be a good estimate of the $N$th fold crest away from a given crest. Simulations (Fletcher & Sherwin 1977) show that $L_d/H$ is a good approximation to $\bar{L}/H$.

It is still useful to approximate the local configuration by the sum of one or two periodic components, but one expects that this approximation will rapidly lose register with the actual layer surface shape with increasing distance from the local structure to which this approximating form is fitted. The qualitative comparison between the low limb-dip folds in Fig. 1(b) and the periodic form in Fig. 2 is an example of this. We therefore consider two simple representations of local fold form where the forms are oblique to the principal axes of the basic-state flow: a cylindrical form, and a doubly-plunging form.

Let axes $x'$ and $y'$ make angles of $\beta$ with the $x$ and $y$ axes, and consider the fold form

$$\zeta(x',y') = A\cos(l'x')\cos(m'y'). \tag{36}$$

Substituting

$$\begin{aligned} x' &= x\cos\beta + y\sin\beta \\ y' &= -x\sin\beta + y\cos\beta \end{aligned} \tag{37}$$

into (36) and expanding, we obtain

$$\begin{aligned} \zeta(x,y) = A/2[&\cos(l_1x)\cos(m_1y) - \sin(l_1x)\sin(m_1y)] \\ &+ A/2[\cos(l_2x)\cos(m_2y) \\ &- \sin(l_2x)\sin(m_2y)], \end{aligned} \tag{38}$$

where

$$\begin{aligned} l_1 &= l'\cos\beta - m'\sin\beta, \quad m_1 = m'\cos\beta + l'\sin\beta \\ l_2 &= l'\cos\beta + m'\sin\beta, \quad m_2 = m'\cos\beta - l'\sin\beta. \end{aligned}$$

Consider first the special case $m' = 0$, which corresponds to a cylindrical, sinusoidal form whose axis makes an angle of $\beta$ with the $y$ axis. In this case, $l_1 = l_2 = l = l'\cos\beta$, and $m_2 = -m_1 = m = l'\sin\beta$, and (38) reduces to

$$\zeta(x,y) = A[\cos(lx)\cos(my) - \sin(lx)\sin(my)]. \tag{39}$$

The growth rates of the two parts of the cylindrical perturbation thus are the same, since both have the same values of $\lambda^2 = l^2 + m^2$ and $m/l = \tan\beta$. This proves that the cylindrical perturbation will retain its form as deformation continues. Of course, just as in the case of the fully two-dimensional situation, the wavenumbers, and hence both the wavelength $L_x'$ and the angle of the fold axis to the $y$ axis, $\beta$, change with continued deformation. Their rates of change are determined from the relations

$$\begin{aligned} \mathrm{d}l/\mathrm{d}t &= -l\bar{\varepsilon}_{xx} \\ \mathrm{d}m/\mathrm{d}t &= -m\bar{\varepsilon}_{yy}, \end{aligned} \tag{40}$$

and the above definitions to be

$$\lambda\mathrm{d}\lambda/\mathrm{d}t = -(l^2\bar{\varepsilon}_{xx} + m^2\bar{\varepsilon}_{yy})$$

and

$$\mathrm{d}(\tan\beta)/\mathrm{d}t = (\bar{\varepsilon}_{xx} - \bar{\varepsilon}_{yy})\tan\beta. \tag{41}$$

These relations would be used to evaluate the cumulative amplification of the perturbation if its growth rate were slow relative to the mean rate of deformation, as in the two-dimensional models of Sherwin & Chapple (1968), Fletcher (1974), or Hudleston & Holst (1984).

It can be seen from the above that the fold hinge behaves like a passive marker in the basic state of flow. We can ask the further distinct question as to whether particles initially on the hinge remain there as the deformation continues. The effect of the basic state of flow considered here is to move all material lines in either the layer or the medium as 'passive markers'. Consequently, if particles initially on the fold hinge move off it, this must arise from the perturbing flow. To answer the question, we first determine the total perturbing velocity for the fold shape (39), and then resolve its components along the axes $x'$, $y'$, $z' = z$.

Notice that the second part of the form (39) is obtained from the first by a phase shift of $\pi/2$ in the $x$ direction, and a phase shift of $-\pi/2$ in the $y$ direction. To obtain the form of the velocity field corresponding to it, we therefore make the following replacements: $\cos(lx)$ by $\cos(lx + \pi/2) = -\sin(lx)$, $\cos(my)$ by $\cos(my - \pi/2) = \sin(my)$, and $\sin(lx)$ by $\cos(lx)$, $\sin(my)$ by $-\cos(my)$. Using these, we obtain the additional parts of the perturbing flow from (18a) and (22a), and after further condensing the trigonometric expressions, we obtain

$$\begin{aligned} \tilde{u} &= [-(l/\lambda)V_p + mV_t]\sin(lx + my) \\ \tilde{v} &= [-(m/\lambda)V_p - lV_t]\sin(lx + my) \\ \tilde{w} &= W_p\cos(lx + my), \end{aligned} \tag{42}$$

where $V_p$ and $V_t$ are the $z$-dependent terms in the poloidal and toroidal flows, respectively. Substituting (42) into the transformation relations

$$\begin{aligned} u' &= u\cos\beta + v\sin\beta \\ v' &= -u\sin\beta + v\cos\beta \\ w' &= w, \end{aligned} \tag{43}$$

and using $l'x' = lx + my$, we find

$$\tilde{u}' = -V_p \sin(l'x')$$
$$\tilde{v}' = -l'V_t \sin(l'x') \quad (44)$$
$$\tilde{w}' = W_p \cos(l'x').$$

Here $l'$ can be replaced by the wavenumber $\lambda$. The relation (44) shows that the perturbing flow for an obliquely-oriented cylindrical perturbation, referred to the instantaneous position of axes $x'$,$y'$ and $z'$, where $y'$ is parallel to the perturbation axis, is the sum of a plane flow $\tilde{u}' = \tilde{u}'(x',z')$, $\tilde{v}' = 0$, $\tilde{w}' = \tilde{w}'(x',z')$ and an anti-plane flow $\tilde{v}' = \tilde{v}'(x',z')$ $\tilde{u}' = \tilde{w}' = 0$. The former is purely poloidal, and the latter is purely toroidal. In particular, since $\tilde{u}'$ is zero at $x' = 0$, particles initially on the fold hinge remain there. (It is perhaps likely that this result could be obtained more simply from an argument based purely on symmetry.) The form of the perturbing flow (44), together with the equivalent expressions in the stress components would be that most convenient for computing principal directions of stress or strain-rate.

From (32) we can estimate the growth rate of an obliquely-inclined cylindrical perturbation in plane strain relative to one oriented normal to the direction of shortening, as in the Appalachian field example. This estimate will be valid if the effect of gravity in suppressing fold growth is not significant, and if the mechanical layers are adequately approximated as linear viscous fluids, even though the layer configurations are different. For the obliquely-oriented cylindrical form whose axis is inclined at a counter-clockwise angle to the $y$ axis, $\beta$, $l = \lambda \cos\beta$ and $m = \lambda \sin\beta$. Then, from (32), $E = (1 + \tan^2\beta)^{-1} + 1$. For $\beta = -30°$, $E = 1.75$. If the fold form with axis parallel to $y$ is amplified by 100, the inclined form will be amplified by a factor $(100)^{1.75/2} = 56$; such a structure will persist during the subsequent deformation.

Now consider the more general case of the obliquely-oriented, non-cylindrical form (38). When $m' \neq 0$, we have $l_1 \neq l_2$ and $m_1 \neq m_2$. Therefore, while $l_1^2 + m_1^2 = l_2^2 + m_2^2 = \lambda^2$, we have $m_1/l_1 \neq m_2/l_2$. Consequently, with further deformation, the form (38) is not preserved, but evolves into

$$\zeta(x,y) = A_1[\cos(l_1x)\cos(m_1y) - \sin(l_1x)\sin(m_1y)]$$
$$= A_2[\cos(l_2x)\cos(m_2y) - \sin(l_2x)\sin(m_2y)], \quad (45)$$

where $A_1$ and $A_2$ both have the initial amplitudes $A/2$, but grow at different rates determined by the values of $m_1/l_1$ and $m_2/l_2$. Evidently, this form can be represented by the sum of two cylindrical forms with axes located at angles of $\beta_1$ and $\beta_2$ from the $y$ axis, where

$$\tan\beta_1 = m_1/l_1$$
$$= (l'\sin\beta + m'\cos\beta)/(l'\cos\beta - m'\sin\beta)$$
$$\tan\beta_2 = m_2/l_2 \quad (46)$$
$$= (l'\sin\beta - m'\cos\beta)/(l'\cos\beta + m'\sin\beta).$$

The evolution of the single cylindrical form has already been discussed. It suffices to add two such forms to follow the evolution of the shape (45).

## CONCLUSIONS

(1) A general solution for the three-dimensional folding of an isotropic, linear viscous layer has been obtained without the necessity of introducing thin-plate approximations. A toroidal flow, with non-vanishing vorticity component normal to the layer, is required to satisfy both shear traction matching conditions. This flow is not coupled with the poloidal flow, which solely determines the rate of fold growth.

(2) The separation constant $\lambda$ for the most rapidly growing component is the same as that obtained for the cylindrical perturbation in a basic state of plane flow. A cylindrical fold form with axis normal to the maximum direction of shortening in the plane of the layer grows most rapidly for all ratios of the in-plane strain rates, $\bar{\varepsilon}_{yy}/\bar{\varepsilon}_{xx} < 1$ as opposed to one with a finite fold aspect ratio, $L_x/L_y$. When $\bar{\varepsilon}_{yy}/\bar{\varepsilon}_{xx} < 0$, components with the same $\lambda$ but different $m/l$ all grow at the same relative rate.

(3) The three-dimensional fold forms shown by the structure contour map of a portion of the central Appalachian Plateau province are well-approximated by the sum of two obliquely-oriented cylindrical forms. The rate of amplification of this structure can be estimated from the present treatment, and the 'earlier' cylindrical components will continue to grow at a substantial rate.

*Acknowledgements*—This research was supported by NSF Grant EAR-8708326. Neil Ribe pointed out to me the decomposition of a velocity field into poloidal and toroidal parts. Reviews by Martin Casey and Subir Ghosh are greatly appreciated.

## REFERENCES

Biot, M. A. 1966. Three-dimensional gravity instability derived from two-dimensional solutions. *Geophysics* **31**, 153–166.

Bisshop, F. E. 1960. On two-dimensional cell patterns. *J. Math. Anal. Applic.* **1**, 373–385.

Cate, A. S. 1962. Subsurface structure of the Plateau region of north-central and western Pennsylvania on top of the Oriskany Formation. Pennsylvania Geological Survey, Fourth Series.

Fletcher, R. C. 1974. Wavelength selection in the folding of a single layer with power-law rheology. *Am. J. Sci.* **274**, 1029–1043.

Fletcher, R. C. 1977. Folding of a single viscous layer: exact infinitesimal amplitude solution. *Tectonophysics* **39**, 593–606.

Fletcher, R. C. 1982. Analysis of the flow in layered viscous fluids at small, but finite amplitude, with application to mullion structures. *Tectonophysics* **81**, 51–66.

Fletcher, R. C. & Sherwin, J.-A. 1977. The relation between fold arc-length and preferred wavelength for single layer folds. *Am. J. Sci.* **278**, 1085–1098.

Ghosh, S. K. 1970. A theoretical study of intersecting fold patterns. *Tectonophysics* **9**, 559–569.

Hudleston, P. J. & Holst, T. B. 1984. Strain analysis and fold shape in a limestone layer and implications for layer rheology. *Tectonophysics* **106**, 321–347.

Johnson, A. M. & Page, B. M. 1976. Part VII, Development of folds within Huasna syncline, San Luis Obispo County, California. *Tectonophysics* **33**, 97–143.

Sherwin, J.-A. 1972. Decollement folding. Unpublished Ph. D. thesis, Brown University.

Sherwin, J.-A. & Chapple, W. M. 1968. Wavelengths of single layer folds: a comparison between theory and observation. *Am. J. Sci.* **266**, 167–179.

Smith, R. B. 1975. Unified theory of the onset of folding, boudinage, and mullion structure. *Bull. geol. Soc. Am.* **86**, 1601–1609.

Smith, R. B. 1977. Formation of folds, boudinage, and mullions in non-Newtonian materials. *Bull. geol. Soc. Am.* **88**, 312–320.

Treagus, S. H. 1973. Buckling stability of a viscous single-layer system, oblique to the principal compression. *Tectonophysics* **19**, 271–289.

Watkinson, A. J. 1975. Multilayer folds initiated in bulk plane strain, with the axis of no change perpendicular to the layering. *Tectonophysics* **28**, T7–T11.

Wiltschko, D. V. & Chapple, W. M. 1977. Flow of weak rocks in Appalachian Plateau folds. *Bull. Am. Ass. Petrol. Geol.* **61**, 653–670.